European Journal of Neuroscience, Vol. 18, pp. 155–163, 2003

Regional differences in the circadian modulation of human sleep spindle characteristics

Vera Knoblauch,[1] Wim Martens,[2] Anna Wirz-Justice,[1] Kurt Kräuchi[1] and Christian Cajochen[1]
[1]Centre for Chronobiology, Psychiatric University Clinic, Wilhelm Klein-Str. 27, 4025 Basel, Switzerland
[2]TEMEC Instruments B.V., Spekhofstraat 2, 6466 LZ Kerkrade, the Netherlands

Keywords: circadian rhythm, fast Fourier transform, fast time frequency transform, melatonin, topography

Abstract

Electroencephalographic oscillations in the sleep spindle frequency range (11–16 Hz) are a key element of human nonrapid eye movement sleep. In the present study, sleep spindle characteristics along the anterior–posterior axis were analysed during and outside the circadian phase of melatonin secretion. Sleep electroencephalograms were recorded during naps distributed over the entire circadian cycle and analysed with two different methodological approaches, the classical fast Fourier transform in the frequency-domain and a new method for instantaneous spectral analysis, the fast time frequency transform that yields high-resolution parameters in the combined time-frequency-domain. During the phase of melatonin secretion, spindle density was generally increased and intraspindle frequency variation reduced. Furthermore, lower spindle frequencies were promoted: peak frequencies shifted towards the lower end of the spindle frequency range, and spindle amplitude was enhanced in the low-frequency range (11–14.25 Hz) and reduced in the high-frequency range (~14.5–16 Hz). The circadian variation showed a clear dependence on brain topography such that it was maximal in the parietal and minimal in the frontal derivation. Our data provide evidence that the circadian pacemaker actively promotes low-frequency sleep spindles during the biological night with a parietal predominance.

Introduction

The timing and structure of human sleep are regulated by the endogenous circadian pacemaker located in the suprachiasmatic nuclei (SCN) of the hypothalamus (Dijk & Czeisler, 1995b; Dijk *et al*., 1997). The strength of this circadian control is very different for the two main electroencephalographic (EEG) oscillations during non-rapid eye movement (NREM) sleep – slow waves and sleep spindles. Slow-wave activity (SWA; EEG power density in the 0.75–4.5 Hz range) does not exhibit substantial circadian modulation, whereas activity in the spindle frequency range (SFA; EEG power density in the 11–16 Hz range) shows a clear circadian rhythm (Dijk & Czeisler, 1995b; Dijk *et al*., 1997). This circadian rhythm is frequency-specific, such that SFA in the 12.25–13 Hz range coincides with the peak, and SFA in the 14.25–15.5 Hz range with the nadir of the endogenous rhythm of melatonin secretion (Dijk *et al*., 1997). This inverse circadian phase relationship in low and high SFA has two possible explanations. The frequency *per se* of sleep spindles could be modulated (i.e. a general slowing of spindle frequencies during the night), or their amplitude and/or duration might exhibit frequency-specific modulation. Indeed, a recent study has demonstrated that frequency, amplitude, as well as the duration of sleep spindles during NREM sleep all varied significantly across the circadian cycle (Wei *et al*., 1999).

The role of sleep spindles is largely unknown. Spindle oscillations originate in the thalamus, which is the major gateway for information flow to the cortex (Steriade *et al*., 1993). Sleep spindles could reduce this sensory transmission and thereby protect the cortex from arousing stimuli (Steriade *et al*., 1993). There is also increasing evidence for an involvement of sleep spindles in synaptic plasticity and memory processes (Siapas & Wilson, 1998; Gais *et al*., 2002; for a review see Sejnowski & Destexhe, 2000).

Spectral analysis of the EEG, the method of choice in sleep research, averages spectral components over the considered time-window and does not discriminate synchronized spindle activity from desynchronized activity in the same frequency band. Therefore, it neither segregates the contribution of changes in frequency from amplitude, nor can it yield time-incidence and time-duration in sleep spindle frequency activity.

It is not yet known whether a frequency-specific circadian modulation of spindle amplitude exists, nor is it known whether circadian modulation of SFA characteristics varies across brain locations. We hypothesized that EEG power density, as well as spindle density (number per time epoch), amplitude and duration show a frequency-specific circadian variation. Furthermore, we hypothesized that the circadian variation of these spindle characteristics depends on brain topography along the antero-posterior axis.

To test these hypotheses, we have applied two methodological approaches to quantify the contribution of spindle amplitude, frequency and density to the circadian as well as topographic modulation of SFA: classical spectral analysis in the frequency-domain (by means of the fast Fourier transform; FFT) and a new method for so-called joint time-frequency domain or instantaneous spectral analysis (by means of the fast time frequency transform; FTFT).

Materials and methods

Study participants

Seventeen healthy volunteers (nine female, eight male, age range 20–31 years, mean ± SEM 25 ± 0.9 years) participated in the study.

Correspondence: Dr Christian Cajochen, as above.
E-mail: christian.cajochen@pukbasel.ch

Received 20 February 2003, revised 16 April 2003, accepted 28 April 2003

doi:10.1046/j.1460-9568.2003.02729.x

All subjects were nonsmokers, free from medical, psychiatric and sleep disorders, as assessed by screening questionnaires, a physical examination and a polysomnographically recorded screening night. Drug-free status was verified through urinary toxicologic analysis. Female subjects were studied during the follicular phase of their menstrual cycle, five of them using oral contraceptives. All participants gave signed informed consent and the study protocol, screening questionnaires and consent form were approved by the local Ethical Committee.

Protocol

During the week preceding the study (baseline week), subjects were instructed to refrain from excessive physical activity, caffeine and alcohol consumption and to maintain a regular sleep–wake schedule (bed- and wake-times within ±30 min of self-selected target time). The latter was verified by a wrist activity monitor (Cambridge Neurotechnologies®, UK) and sleep logs. The timing of their sleep–wake schedule was calculated in such a way that the 8-h sleep episode was centred at the midpoint of each subject's habitual sleep episode as assessed by actigraphy and sleep logs during the baseline week. After the baseline week, subjects reported to the laboratory in the evening and spent an 8-h sleep episode, followed by 16 h of scheduled wakefulness to adjust to the <8 lux experimental conditions (Day 1; Fig. 1). After a second 8-h sleep episode (baseline night), subjects underwent a 40-h short sleep–wake cycle paradigm under constant posture conditions (near recumbent during wakefulness and supine during scheduled sleep episodes) during which they completed 10 alternating cycles of 75 min of scheduled sleep (light levels: 0 lux) and 150 min of scheduled wakefulness. The wake episodes were spent under constant routine conditions (constant dim light levels <8 lux, constant posture, food and liquid intake at regular intervals, no time cues; for details of the CR method see (Cajochen *et al.*, 1999). The protocol ended with an 8-h recovery sleep episode. Results from the baseline and recovery night have been reported elsewhere (Knoblauch *et al.*, 2002).

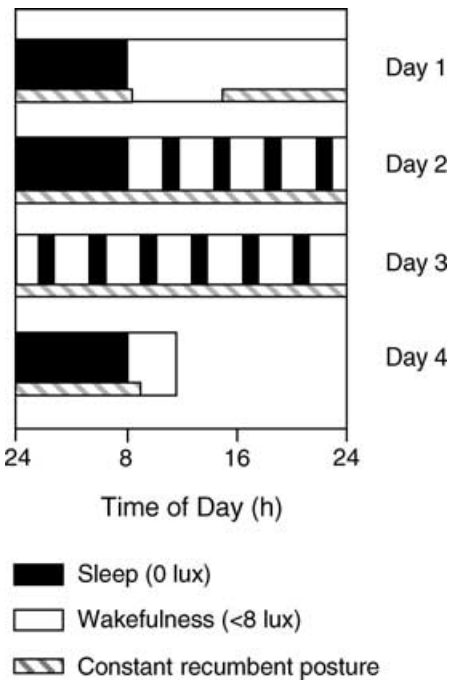

FIG. 1. Overview of the protocol design. After 2 nights and a day in the laboratory to adapt, a 40-h short sleep–wake cycle paradigm (75/150 min) under constant posture was carried out, followed by an 8-h recovery night. Black bars indicate scheduled sleep episodes (light levels 0 lux); white bars indicate scheduled episodes of wakefulness (light levels <8 lux); hatched bars indicate controlled posture (semirecumbent during wakefulness and supine during scheduled sleep).

Sleep recordings and analysis

Sleep was recorded polysomnographically using the VITAPORT digital ambulatory sleep recorder (Vitaport-3 digital recorder, TEMEC Instruments B.V., Kerkrade, the Netherlands). Twelve EEGs, two electro-oculograms, one submental electromyogram and one electrocardiogram signal were recorded. All signals were filtered at 30 Hz (4th order Bessel type anti-aliasing low-pass filter, total 24 dB/Oct) and a time constant of 1.0 s was used before online digitization (range 610 μV, 12-bit AD converter, 0.15 μV/bit; sampling rate at 128 Hz for the EEG). The raw signals were stored online on a Flash RAM Card (Viking, USA) and downloaded offline to a PC hard drive. Sleep stages were visually scored on a 20-s basis (Vitaport Paperless Sleep Scoring Software) according to standard criteria (Rechtschaffen & Kales, 1968) and all further quantitative spindle analyses were limited to sleep stage two.

EEG spectral analysis

All EEGs were subjected to spectral analysis using an FFT (10% cosine 4-s window) resulting in a 0.25-Hz bin resolution. In parallel, EEG artifacts were detected by an automated artifact detection algorithm (CASA, 2000 PhyVision B.V., Gemert, the Netherlands). For final data reduction, the artifact-free 4-s epochs were averaged over 20-s epochs.

EEG power spectra were calculated during stage two in the frequency range from 0.5 to 32 Hz. Here, we report EEG data derived from the midline (Fz, Cz, Pz, Oz) referenced against linked mastoids (A1, A2) in the range of 0.5–25 Hz.

EEG instantaneous spectral analysis

The same digitized EEGs were subjected to instantaneous spectral analysis using the FTFT (Martens, 1992). For the EEG, the FTFT calculates instantaneous amplitude, frequency and bandwidth in eight frequency bands from 0–4 Hz, 4–8 Hz, . . ., 28–32 Hz. Instantaneous bandwidth is computed from the instantaneous frequency as the rectified first derivative with respect to time. Therefore, the higher the frequency variability, the higher the bandwidth. Based on the 4 Hz range of the filters, the resolution in time of the above parameters is 0.125 s. Over a moving template of 1 s duration, thresholds are applied to amplitude, frequency and bandwidth parameters to differentiate synchronized activity from ongoing noise as well as to remove artifacts (Martens, 1999). The thresholds were determined empirically on a learning-set of EEG recordings to yield the closest possible agreement with visual scores. Incorporating the instantaneous bandwidth helped to achieve a closer agreement in comparison with using only an amplitude threshold. Finally, the optimized settings from the learning set were applied to the data set of this study. Here, we focus on detected synchronized spindle activity. Spindles were detected from the outcome of the 8–12 Hz and 12–16 Hz frequency band, but the frequency and bandwidth threshold for spindle detection were limited to the range of 11–16 Hz. These thresholds again were determined empirically and compared with the visual score. Furthermore, a duration limit (0.5 s and 2 s) was applied for detected spindles. As a result, we obtained the amplitude and frequency of each individual spindle at a time-resolution of 0.125 s. The frequency resolution was 0.25 Hz. In other words, for each 0.25 Hz frequency bin between 11 and 16 Hz, the time incidence (corresponds to the number of 0.125-s epochs within

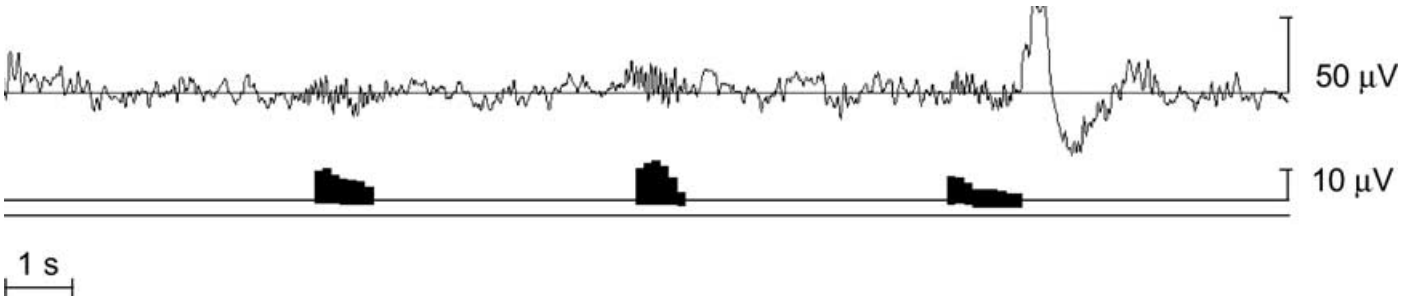

FIG. 2. Raw EEG signal (above) and the output of the fast time frequency transform (FTFT, below) derived from Pz during a 20-s epoch of stage two sleep. The FTFT depicts synchronized spindle activity, subdivides each spindle into 0.125-s epochs (each represented by a black horizontal bar) and computes frequency and amplitude for each 0.125-s epoch separately. The height of a horizontal bar reflects the mean amplitude (μV), the position relative to the horizontal lines reflects the mean frequency within a 0.125-s epoch. The upper horizontal line is at 12 Hz, the lower at 16 Hz.

the given frequency bin) and the amplitude in these 0.125-s epochs was calculated. Figure 2 depicts a raw EEG curve together with the output of the spindle FTFT. For each 20-s epoch of stage two sleep, the mean time incidence and amplitude of synchronized spindle frequency activity were computed per 0.25-Hz frequency bin between 11 and 16 Hz. Furthermore, spindle density (number of sleep spindles/20-s epoch) was calculated. Finally, for each individual spindle, the following parameters were computed: duration, mean frequency, mean amplitude, standard deviation of frequency, frequency at onset and offset.

To compare spindle detection of this method with other spindle detection techniques, spindle density in Cz was calculated during the baseline night of this protocol. The value obtained (2.0176 n/20 s ± 0.23) was very similar to spindle density in central derivations (C3, C4 or Cz) reported in other studies using automated (Dijk *et al*., 1993; Wei *et al*., 1999) or visual (De Gennaro *et al*., 2000) spindle detection algorithms. Furthermore, detected synchronized spindle activity (Fig. 2) was verified visually by one rater (V.K.). Because we used a relatively low amplitude threshold (3–5 μV template) and a relatively broad frequency range (11–16 Hz), the algorithm detected a spindle density slightly higher than if scored visually. The thresholds for spindle detection were deliberately set such that the algorithm yielded more spindles than when scored visually; this is particularly important in the presence of delta waves where the human eye often misses superimposed sleep spindles.

Salivary melatonin

Saliva was collected at ∼30 min intervals during scheduled wakefulness. Saliva samples were assayed for melatonin using a direct double-antibody radioimmunoassay validated by gas chromatography–mass spectroscopy with an analytical least detectable dose of 0.15 pg/mL and a functional least detectable dose of 0.65 pg/mL (Bühlmann Laboratories, Schönenbuch, Switzerland; Weber *et al*., 1997).

Classification of naps

Naps comprising a total stage two duration of <5 min were excluded from the analysis. The first 75 min after lights off in the recovery night were considered as an additional nap. For time course analyses, naps 4 and 10 were excluded because too few subjects fulfilled these criteria of a stage two duration of at least 5 min (five and three subjects, respectively), whereas a total of nine subjects fulfilled these criteria in the remaining naps.

The top left hand panel in Fig. 3 illustrates the timing of the scheduled naps across the protocol in relation to endogenous melatonin secretion. Naps were classified into night naps and day naps depending on their occurrence during, or outside, melatonin secretory phase. This was defined as follows. The 24-h mean melatonin concentration (between hours 5 and 29 of the 40-h nap protocol) was calculated for each subject as an individual threshold level. The mean overall threshold was 9.1 ± 1.4 pg/mL (mean ± SEM; $n = 17$) and is indicated as a horizontal line in the top left hand panel in Fig. 3. A nap was rated as a night nap if the melatonin concentration of the last saliva sample before the nap was above the threshold; otherwise, it was rated as a day nap. There were on average 5.76 ± 0.39 day naps and 2.94 ± 0.2 night naps per subject. The duration of stage two sleep did not differ significantly between day and night naps ($F_{1,16} = 0.2$; $P = 0.7$).

Statistics

The statistical packages SAS® (SAS Institute Inc., Cary, NC, USA; Version 6.12) and Statistica® (StatSoft Inc., 2000. STATISTICA for Windows, Tulsa, OK, USA) were used. For day–night comparisons, averaged values across daytime naps were compared with averaged values across night-time naps. For time course analyses, data derived from the spectral analysis were subjected to two-way analyses of variance for repeated measures (rANOVA) with the factors Derivation and Nap. For day–night comparisons, two-way rANOVAs with the factors Derivation and Condition or three-way rANOVAs with the factors Condition, Derivation and Frequency bin (for the time incidence and amplitude per 0.25 Hz bin) were used. All *P*-values derived from rANOVAs were based on Huynh–Feldt's (H-F) corrected degrees of freedom, but the original degrees of freedom are reported. For *post hoc* comparisons the Duncan's multiple range test and *t*-tests with correction for multiple comparisons (Curran-Everett, 2000) were used.

Results

Spectral analysis (FFT)

Time course

Figure 3 illustrates the timing of the scheduled naps across the protocol in relation to endogenous melatonin secretion (top left hand panel) and the dynamics of EEG power density across naps (relative stage two spectra of each nap, expressed as a percentage of the mean of all naps) in the range of 0.5–25 Hz in Pz. In the insets, the corresponding absolute spectra between 11 and 16 Hz are shown (spectra of the individual nap together with the mean spectra of all naps). Successive naps (without nap 4 and 10, see Methods) are plotted one below another in two columns, whereby naps occurring at similar circadian times are placed next to each other. Visual inspection reveals a prominent time-dependent modulation in the spindle frequency range. A one-way rANOVA with the factor Nap was performed and revealed

that power density in most frequency bins between 9 and 21.75 Hz varied significantly across naps (see symbols above the top right hand panel of Fig. 3). By contrast, power density between 0.5 and 9 Hz, thus in the delta, theta and lower alpha range, as well as above 21.75 Hz did not exhibit a significant modulation over time. For frequency bins with a significant rANOVA, *post hoc* comparisons between the value for the individual nap and the mean of all naps were performed (Duncan's multiple range test on log-transformed absolute values). In general,

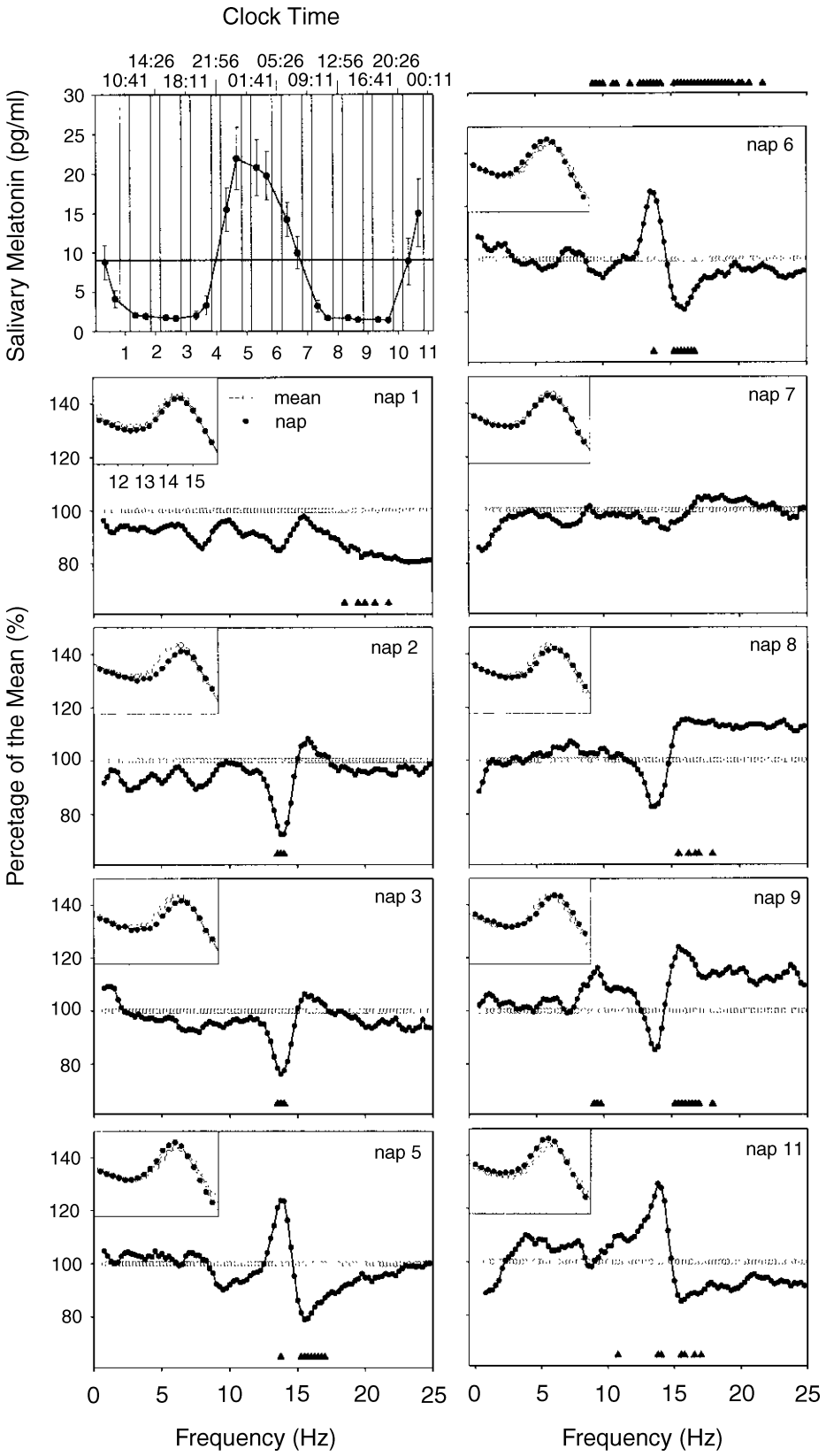

FIG. 3. Melatonin secretion, timing of the naps and the time course of EEG power density in the naps (nap 1–3, 5–9 and 11). *Top left hand panel*: Black symbols represent the mean curve of melatonin secretion (mean ± SEM; $n = 17$). The horizontal line marks the mean threshold (calculated as the 24 h mean melatonin concentration). Vertical grey bars represent nap 1–11. Average times, when the midpoint of the naps occurred, are indicated on the top horizontal axis (mean times, $n = 17$). *Other panels*: EEG power density in the range from 0.5 to 25 Hz in nap 1–11 (without nap 4 and 10) expressed as a percentage of the mean of all naps (except nap 4 and 10) for Pz (mean ± SEM; $n = 9$). Symbols above the top right hand panel (nap 6) indicate frequency bins for which the factor Nap was significant ($P < 0.05$; one-way rANOVA on log transformed absolute values). Triangles near the abscissa indicate a significant difference between the value for the respective nap and the mean of all naps in these frequency bins ($P < 0.05$; Duncan's multiple range test on log transformed absolute values). *Insets:* original absolute spectra between 11 and 16 Hz (spectra of the individual nap (●); mean spectra of all naps (o); mean, $n = 9$).

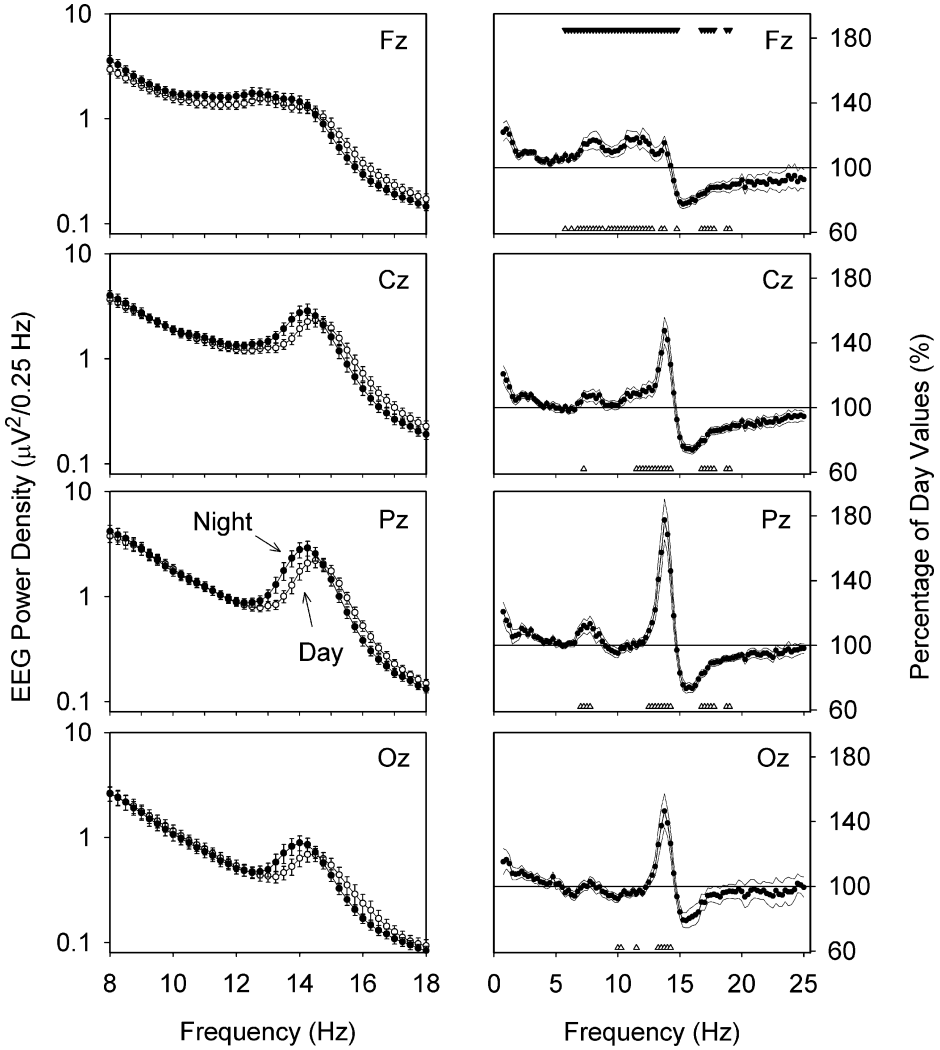

FIG. 4. EEG power density per 0.25-Hz bin for the midline derivations (Fz, Cz, Pz, Oz) during stage two (mean ± SEM; $n = 17$). *Left hand panels*: Absolute EEG power density between 8 and 18 Hz for the night naps (●) and the day naps (○). *Right hand panels*: Relative night spectra (expressed as percentage of day values) between 0.5 and 25 Hz. Symbols at the top of the top panel indicate frequency bins for which the interaction between Derivation and Condition was significant ($P < 0.05$; rANOVA on log transformed absolute values). Triangles near the abscissa indicate a significant difference between day and night in these frequency bins ($P < 0.05$; paired *t*-test corrected for multiple comparisons).

power density was reduced in the lower spindle frequency range and enhanced in the higher frequency range in naps 2, 3, 8 and 9, i.e. in naps occurring when melatonin was not secreted. In naps occurring when melatonin was secreted (i.e. naps 5, 6 and 11), power density was enhanced in the lower spindle frequency range and reduced in the higher frequency range (see Fig. 3 for frequency bins with a significant difference from the mean). The absolute spectra in the insets help to illustrate that the opposite day- and night-time peaks in the low- and high frequency range come about by a shift in the absolute power spectra towards lower frequencies during the night.

Day–night difference

In a next step, the spectra of naps occurring during melatonin secretion (night naps) were compared with the spectra of naps occurring outside melatonin secretion (day naps; see Methods section). The left-hand panel in Fig. 4 shows mean absolute EEG power density between 8 and 18 Hz during night and day naps. Visual inspection reveals more power in the spindle peak during the night than during the day, and the curves are shifted towards lower frequencies relative to the day spectra. For better visualization of this day–night difference, the spectra of the night naps are expressed as a percentage of the day nap spectra in the range from 0.5 to 25 Hz (Fig. 4, right-hand panels). The interaction between Derivation (Fz, Cz, Pz, Oz) and Condition (day, night) was significant in the following frequency ranges: 5.5–14.75 Hz, 16.5–17.75 Hz and 18.5–19 Hz (P at least < 0.05; rANOVA).

There was a pronounced and significant nocturnal increase of EEG power density in Cz, Pz and Oz in the following frequency ranges: between 11.25 and 14.25 Hz in Cz; between 12.25 and 14.25 Hz in Pz; and between 13 and 14.25 Hz in Oz ($P < 0.05$, day vs. night; paired *t*-test corrected for multiple comparisons). In Fz, the increase (significant between 11 and 12.75 and 13.25 and 13.75 Hz) was less distinct and also spanned to adjacent lower frequency ranges, i.e. the alpha and theta range (see Fig. 4). The increase was maximal in the 13.5–13.75 Hz bin and was significantly higher in Pz than in Cz, Oz and Fz, as well as significantly lower in Fz than in the other three derivations (Derivation, $F_{3,48} = 42.3$, $P < 0.01$, rANOVA; Duncan's multiple range test, $P < 0.0001$). The nocturnal reduction of EEG power density in the higher spindle frequency range (>14.75 Hz) did not depend on derivation (no significant interaction between Derivation and Condition in the 14.75–16.5 Hz range).

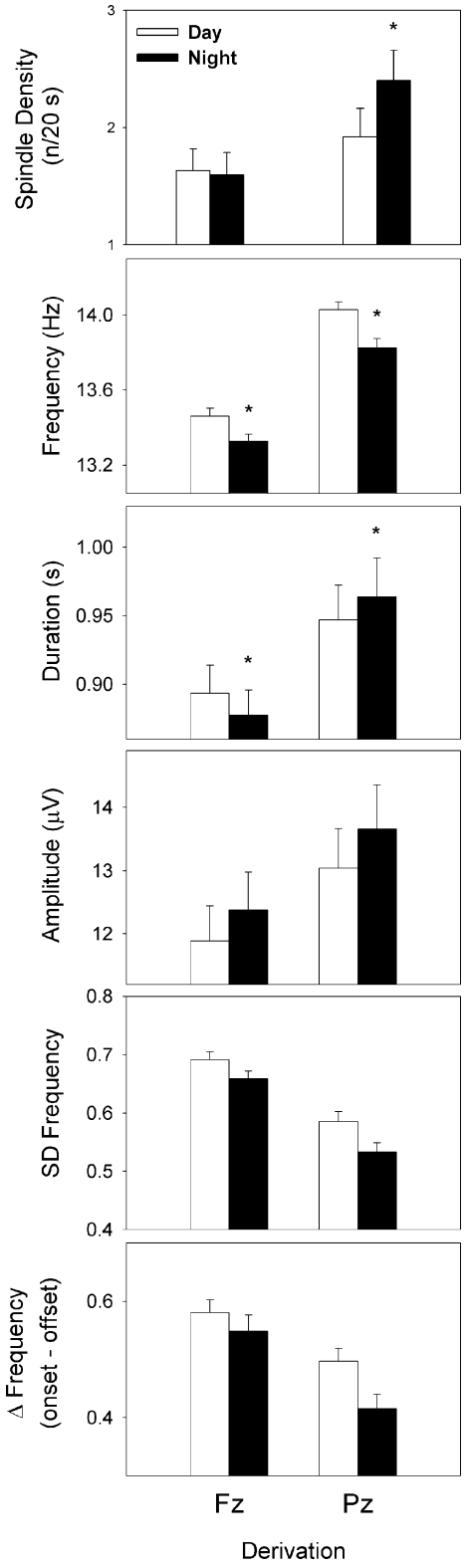

FIG. 5. Mean density (number of sleep spindles per 20-s epoch of stage two), frequency, duration, amplitude, standard deviation of frequency (SD Frequency, intraspindle frequency variability), and difference between onset and offset frequency (Δ Frequency) of sleep spindles during night naps (black bars) and day naps (white bars) for the frontal (Fz) and parietal (Pz) derivation (mean ± SEM; $n = 17$). Asterisks indicate a significant difference between day and night ($P < 0.05$; Duncan's multiple range test).

Instantaneous frequency analysis (FTFT)

Spindle density and spindle parameters

Spindle density (number of spindles/20 s epoch), duration, frequency, amplitude, standard deviation of frequency (SD Frequency), frequency at onset, frequency at offset and the difference between frequency at onset and frequency at offset (Δ Frequency) were calculated (Fig. 5). A two-way rANOVA with the factors Condition and Derivation was performed for each of these variables (Table 1). The interaction between these two factors yielded significance for spindle density, frequency and duration. *Post hoc* comparison revealed that spindle density was significantly higher during the night than during the day in Pz ($P < 0.001$, Duncan's multiple range test), whereas in Fz, no significant day–night difference was observed. Spindle frequency was significantly lower during the night than during the day in both Fz and Pz (Fig. 5; $P < 0.05$, Duncan's multiple range test). Spindle duration was shorter during the night in Fz, and higher during the night than during the day in Pz (Fig. 5; $P < 0.05$, Duncan's multiple range test). The main factor Derivation was significant for all variables, the main factor Condition for all variables except for spindle duration. Spindle amplitude was significantly higher during the night than during the day and significantly higher in Pz than in Fz. SD Frequency, a measure for intraspindle frequency variability, was significantly higher during the day than during the night, and significantly higher in Fz than in Pz (Fig. 5). In both derivations and during both conditions (day, night), onset frequency was significantly higher than offset frequency (Variable × Derivation, $F_{1,16} = 12.9$, $P < 0.01$, rANOVA; Variable × Condition, $F_{1,6} = 6.3$, $P < 0.05$, rANOVA; Duncan's multiple range test, $P < 0.001$, data not shown), i.e. frequency within a spindle generally slowed down. The extent of this frequency reduction (expressed as Δ Frequency, the difference between onset and offset frequency) was however, significantly higher in Fz than in Pz and significantly higher during the day than during the night (Fig. 5). The smaller intraspindle downward frequency modulation during the night than during the day implies an unequal reduction of onset and offset frequency during the night. To test this, onset and offset frequency at night were expressed as a percentage of onset and offset frequency during the day (relative onset and offset frequency). In Fz, there was no significant difference between the relative onset and offset frequency, whereas in Pz, the onset frequency during the night was significantly more reduced than the offset frequency ($F_{1,16} = 11.6$, $P < 0.005$, rANOVA).

Time incidence per 0.25 Hz frequency bin

The upper panels of Fig. 6 depict the time incidence per 0.25 Hz bin in the 11–16 Hz range. A three-way rANOVA Derivation × Condition × Frequency bin revealed a significant interaction between these factors ($F_{19,304} = 11.7$; $P < 0.0001$). There was a pronounced day-night difference in time incidence in Pz. The curve was shifted towards lower frequencies during the night, resulting in a significant increase in the low and middle spindle frequency range and significant reduction in the upper frequency range ($P < 0.05$, Duncan's multiple range test; see Fig. 6 for exact frequency ranges). In Fz, there was not such a shift between the curves, and they did not differ significantly up to 14 Hz. A significant reduction, however, was found in the upper frequency range (between 14 and 14.75 Hz) during the night ($P < 0.05$, Duncan's multiple range test).

Amplitude per 0.25 Hz frequency bin

The amplitude per 0.25 Hz bin in the 11–16 Hz range is illustrated in the bottom panels of Fig. 6. The interaction between Derivation, Condition and Frequency bin was significant ($F_{19,304} = 5.1$;

TABLE 1. Two-way rANOVA with the factors Condition and Derivation for spindle density (n/20 s), duration, frequency, amplitude, standard deviation of frequency (SD Frequency), onset frequency, offset frequency, and difference between onset and offset frequency of sleep spindles

	Condition		Derivation		Condition × Derivation	
Variable	$F_{1,16}$-value	P-value*	$F_{1,16}$-value	P-value*	$F_{1,16}$-value	P-value*
Density	20.56	< 0.001	16.93	< 0.001	111.83	< 0.0001
Duration	0.01	0.939	25.12	< 0.001	12.29	< 0.01
Mean frequency	81.76	< 0.001	132.92	< 0.001	5.38	< 0.034
Mean amplitude	19.05	< 0.001	11.25	< 0.01	1.13	0.303
SD frequency	30.39	< 0.001	72.12	< 0.001	3.16	0.1
Onset frequency	57.52	< 0.001	100.39	< 0.001	3.72	0.072
Offset frequency	54.18	< 0.001	135.27	< 0.001	0.36	0.556
Frequency difference	6.26	< 0.05*	12.92	< 0.01	2.26	0.15

*P-values < 0.05 were considered significant.

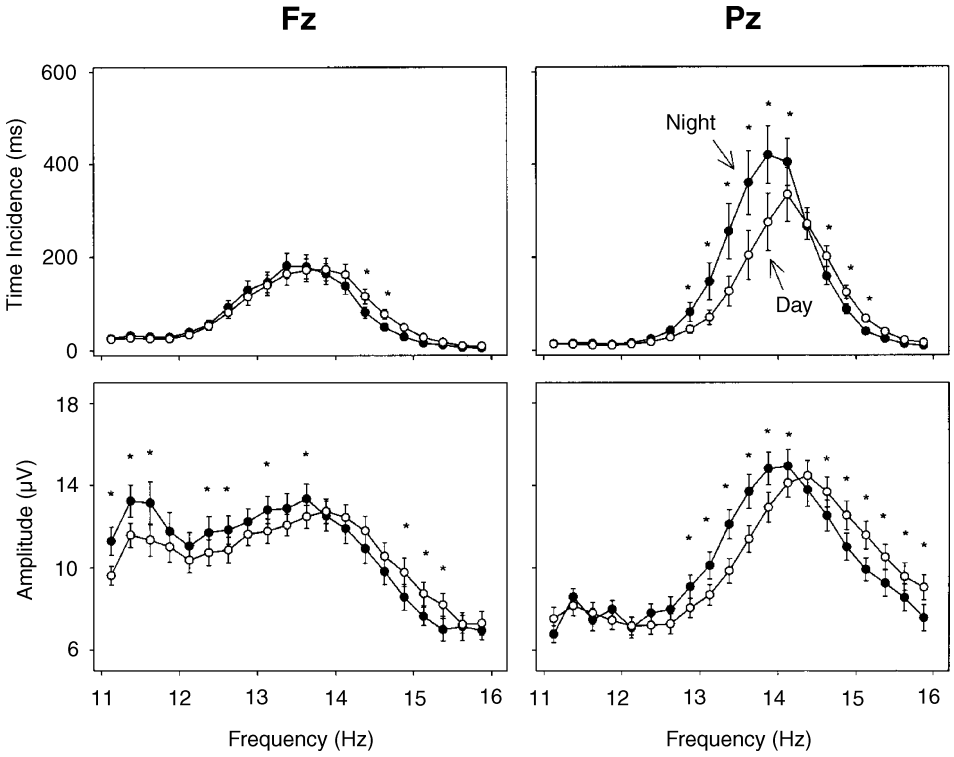

FIG. 6. Time incidence (per 20-s epoch stage two, above) and amplitude (below) per 0.25 Hz bin from 11 to 16 Hz during night naps (●) and day naps (○); mean ± SEM; $n = 17$. Asterisks indicate significant day–night differences ($P < 0.05$; Duncan's multiple range test).

$P < 0.0001$, rANOVA). In both derivations, the night curve was shifted towards lower frequencies relative to the day curve. The amplitude at night was increased in the low frequency range and reduced in the higher frequency range (for statistics see Fig. 6). The peak amplitude, in the range between 13.5 and 14.5 Hz, was less distinct in Fz, where a second peak in the very low frequency range (between 11 and 12 Hz) occurred.

Discussion

The new combined high-time and high-frequency resolution spindle analysis showed that density, frequency and amplitude of sleep spindles vary with the circadian phase of endogenous melatonin secretion and revealed a shift of sleep spindles to lower frequencies concomitant with a higher amplitude in this frequency range during the night. Circadian modulation of sleep spindle characteristics was not uniform along the antero-posterior axis, but showed a parietal maximum.

Furthermore, we show that during the biological night, sleep spindles were more stable in terms of reduced intraspindle frequency variability. We found a general downward trend in frequency within sleep spindles; spindle frequency at the end of the spindle was always lower than at the beginning, but this intraspindle downward frequency modulation was reduced during the night.

The shift towards lower frequencies during the subjective night (when melatonin is secreted) comprised both time incidence and amplitude. This confirms and extends previous data which demonstrated a tight temporal association between the endogenous melatonin rhythm and the circadian profile of sleep spindle activity in the low frequency range (12.25–13 Hz; Dijk *et al.*, 1997). It is known that administration of both a classical hypnotic such as a benzodiazepine or (to a lesser extent) daytime melatonin both enhance spindle frequency

activity particularly in the low frequency range (12.25–14 Hz (Johnson *et al.*, 1976; Borbély *et al.*, 1985; Trachsel *et al.*, 1990; Brunner *et al.*, 1991; Dijk *et al.*, 1995). This has led to the hypothesis that the frequency-specific circadian modulation of SFA is a mechanism to reduce sensory sensitivity and thus favour sleep at the phase of normal sleep time (Dijk & Czeisler, 1995a; Dijk *et al.*, 1997). As yet, there are no experimental data demonstrating a decrease in sensory throughput associated with reduced spindle frequency that might support this hypothesis

We have evidence that the variation of sleep pressure across naps was only moderate. Slow-wave activity, a measure for the level of homeostatic sleep pressure during sleep, did not show a substantial or significant variation over time (Fig. 3). In addition, frontal low EEG activity during wakefulness, a marker of the homeostatic buildup of sleep pressure during wakefulness, exhibited only small changes in the time course of this protocol (Cajochen *et al.*, 2001). These data demonstrate that we were successful in keeping sleep pressure generally low during the 40 h and supports the assumption that, although the influence of homeostatic sleep pressure cannot be excluded completely, the effects reported here mainly reflect the influence of circadian phase. Thus, our data further quantify the sleep spindle-promoting action of the circadian pacemaker. It is still unknown whether the spindle-generating thalamocortical network is influenced directly by the SCN through neuronal pathways, or rather indirectly, through other output variables of the circadian system. Direct projections from the SCN to the thalamus (the paraventricular thalamic nucleus) have recently been reported in rats (Novak *et al.*, 2000). The SCN has indirect projections to the the ventrolateral preoptic nucleus (VLPO) via the dorsomedial hypothalamus (Chou *et al.*, 2002). The VLPO is crucial for NREM sleep promotion (Sherin *et al.*, 1996) and has reciprocal inhibitory connections with wake-promoting neurons in the basal forebrain and brainstem nuclei (reviewed by Saper *et al.*, 2001 and Pace-Schott & Hobson, 2002). Among these, the pedunculopontine and laterodorsal tegmental nucei (PPT-LDT) send direct cholinergic projections to the reticular thalamic nucleus (Berendse & Groenewegen, 1990, 1991), which is thought to play a key role in the regulation of thalamocortical transmission and to be the initial site in the sleep spindle-generating network (Steriade *et al.*, 1993). This could be one possible neuronal pathway for the circadian signal from the SCN to the sleep spindle generating system in the thalamus. Alternatively, the circadian modulation of sleep spindles might be mediated indirectly, via other output variables of the circadian pacemaker, such as melatonin. There is, however, a debate on whether the changes in the EEG power spectra that occur across the circadian cycle are based on the concomitant changes in body (and brain) temperature, reflecting a nonspecific effect of temperature, rather than a sleep-regulatory mechanism under circadian control (Deboer & Tobler, 1995, 1998). Electroencephalogram frequencies slow down with a temperature coefficient (Q_{10}) of approximately 2.5 (Deboer & Tobler, 1995); thus low brain temperature at night could be responsible for the shift of SFA in the power spectra towards lower frequencies. To test this hypothesis, Dijk (1999) compared the EEG power spectra from two time points during a forced desynchrony protocol, one in the morning and one in the evening, where body temperature was nearly identical. Low spindle frequency activity was enhanced markedly in the evening, after the evening increase of plasma melatonin levels, compared with the morning, where plasma melatonin levels were low. Consequently, the circadian variation of EEG spindle frequency activity is unlikely to be caused by changes in body temperature.

Our data demonstrate for the first time that the circadian modulation of sleep spindle characteristics varies with brain location. The most marked difference in the extent of circadian modulation is between frontal and parietal SFA. Frequency differences in frontal and parietal spindles during nocturnal sleep have been demonstrated previously (Gibbs & Gibbs, 1950; Werth *et al.*, 1997; Zeitlhofer *et al.*, 1997; Zygierewicz *et al.*, 1999; Anderer *et al.*, 2001; Finelli *et al.*, 2001). Frontal spindles were found to have a lower frequency (around 12 Hz) than parietal spindles (around 14 Hz) and these findings were interpreted as indication for the existence of two separate types of sleep spindles. It is, however, still not known whether frontally and parietally scalp-recorded sleep spindles originate from two functionally distinct thalamic sources. Spindle oscillations presumably originate in the nucleus reticularis of the thalamus, and are transferred via inhibitory GABAergic projections to thalamocortical neurons in other thalamic nuclei (Steriade *et al.*, 1993). As a result, sleep spindles can be recorded from distant sites in the dorsal thalamus (Contreras *et al.*, 1997). Because the spindle-generating network includes various reciprocal connections between the thalamus and the cortex, the cortical distribution of sleep spindles might probably reflect activities of corresponding nuclei within the dorsal thalamus. Thus differences, e.g. in frequency or in circadian regulation, between frontally and parietally scalp-recorded sleep spindles, do not necessarily imply two distinct spindle generators, but could represent a topography-dependent modulation of one single type of spindle oscillations, whose origin can be traced back to the thalamic reticular nucleus from where is dispersed to distant sites within the thalamus. It remains to be elucidated whether this topography-dependent modulation is related to distinct functional roles – such as memory consolidation and sleep protection – of sleep spindles in these brain regions.

We have recently reported frequency-specific topographical changes within the spindle frequency range after manipulation of sleep pressure (Knoblauch *et al.*, 2002). Thus, both circadian and homeostatic processes affect specific frequencies within the spindle frequency range and this in turn depends on brain region. These results emphasize the highly local and frequency-specific nature of sleep spindle regulation.

Conclusions

The present data show that the close temporal association between the melatonin secretory phase ('biological night') and sleep spindle characteristics clearly depends on brain topography. They provide further evidence for a brain region-specific modulation of sleep spindles, which is regulated by the endogenous circadian pacemaker, and strengthens the potential role of sleep spindles as a mechanism by which the SCN facilitates sleep consolidation.

Acknowledgements

We thank Claudia Renz, Giovanni Balestrieri and Marie-France Dattler for their help in data acquisition, Drs Alexander Rösler and Tobias Müller for medical screenings, and the subjects for participating. This research was supported by Swiss National Foundation Grants START #3130–054991.98 and #3100–055385.98 to C.C. We thank Bühlmann Laboratories, Schöneribuch, Switzerland for their continuous support.

Abbreviations

Δ Frequency, difference between frequency at onset and frequency at offset; EEG, electroencephalogram; FFT, fast Fourier transform; FTFT, fast time frequency transform; NREM, non-rapid eye movement; PPT-LDT, pedunculopontine and laterodorsal tegmental nucei; rANOVA, analyses of variance for repeated measures; SCN, suprachiasmatic nuclei; SD Frequency, standard deviation of frequency; SFA, spindle frequency activity; SWA, slow-wave activity; VLPO, ventrolateral preoptic nucleus.

References

Anderer, P., Klösch, G., Gruber, G., Trenker, E., Pascual-Marqui, R.D., Zeitlhofer, J., Barbanoj, M.J., Rappelsberger, P. & Saletu, B. (2001) Low-resolution brain electromagnetic tomography revealed simultaneously active frontal and parietal sleep spindle sources in the human cortex. *Neuroscience*, **103**, 581–592.

Berendse, H.W. & Groenewegen, H.J. (1990) Organization of the thalamostriatal projections in the rat, with special emphasis on the ventral striatum. *J. Comp. Neurol.*, **299**, 187–228.

Berendse, H.W. & Groenewegen, H.J. (1991) Restricted cortical termination fields of the midline and intralaminar thalamic nuclei in the rat. *Neuroscience*, **42**, 73–102.

Borbély, A.A., Mattmann, P., Loepfe, M., Strauch, I. & Lehmann, D. (1985) Effect of benzodiazepine hypnotics on all-night sleep EEG spectra. *Hum. Neurobiol.*, **4**, 189–194.

Brunner, D.P., Dijk, D.J., Münch, M. & Borbèly, A.A. (1991) Effect of zolpidem on sleep and sleep EEG spectra in healthy young men. *Psychopharmacology*, **104**, 1–5.

Cajochen, C., Khalsa, S.B.S., Wyatt, J.K., Czeisler, C.A. & Dijk, D.J. (1999) EEG and ocular correlates of circadian melatonin phase and human performance decrements during sleep loss. *Am. J. Physiol. Regul. Integr. Comp. Physiol.*, **277**, R640–R649.

Cajochen, C., Knoblauch, V., Kräuchi, K., Renz, C. & Wirz-Justice, A. (2001) Dynamics of frontal EEG activity, sleepiness and body temperature under high and low sleep pressure. *Neuroreport*, **12**, 2277–2281.

Chou, T.C., Bjorkum, A.A., Gaus, S.E., Lu, J., Scammell, T.E. & Saper, C.B. (2002) Afferents to the ventrolateral preoptic nucleus. *J. Neurosci.*, **22**, 977–990.

Contreras, D., Destexhe, A., Sejnowski, T.J. & Steriade, M. (1997) Spatiotemporal patterns of spindle oscillations in cortex and thalamus. *J. Neurosci.*, **17**, 1179–1196.

Curran-Everett, D. (2000) Multiple comparisons: philosophies and illustrations. *Am. J. Physiol. Regul. Integr. Comp. Physiol.*, **279**, R1–R8.

De Gennaro, L., Ferrara, M. & Bertini, M. (2000) Effect of slow-wave sleep deprivation on topographical distribution of spindles. *Behav. Brain Res.*, **116**, 55–59.

Deboer, T. & Tobler, I. (1995) Temperature dependence of EEG frequencies during natural hypothermia. *Brain Res.*, **670**, 153–156.

Deboer, T. & Tobler, I. (1998b) The effects of moderate body temperature changes on the sleep EEG. *Sleep*, **21** (Suppl.), 40.

Dijk, D.J. (1999) Circadian variation of EEG power spectra in NREM and REM sleep in humans: dissociation from body temperature. *J. Sleep Res.*, **8**, 189–195.

Dijk, D.J. & Czeisler, C.A. (1995a) Circadian control of the EEG in non REM sleep. *Sleep Res.*, **24**, 518.

Dijk, D.J. & Czeisler, C.A. (1995b) Contribution of the circadian pacemaker and the sleep homeostat to sleep propensity, sleep structure, electroencephalographic slow waves, and sleep spindle activity in humans. *J. Neurosci.*, **15**, 3526–3538.

Dijk, D.J., Hayes, B. & Czeisler, C.A. (1993) Dynamics of electroencephalographic sleep spindles and slow wave activity in men: effect of sleep deprivation. *Brain Res.*, **626**, 190–199.

Dijk, D.J., Roth, C., Landolt, H.P., Werth, E., Aeppli, M., Achermann, P. & Borbély, A.A. (1995) Melatonin effect on daytime sleep in men: suppression of EEG low frequency activity and enhancement of spindle frequency activity. *Neurosci. Lett.*, **201**, 13–16.

Dijk, D.J., Shanahan, T.L., Duffy, J.F., Ronda, J.M. & Czeisler, C.A. (1997) Variation of electroencephalographic activity during non-rapid eye movement and rapid eye movement sleep with phase of circadian melatonin rhythm in humans. *J. Physiol.*, **505**, 851–858.

Finelli, L.A., Borbély, A.A. & Achermann, P. (2001) Functional topography of the human nonREM sleep electroencephalogram. *Eur. J. Neurosci.*, **13**, 2282–2290.

Gais, S., Mölle, M., Helms, K. & Born, J. (2002) Learning-dependent increases in sleep spindle density. *J. Neurosci.*, **22**, 6830–6834.

Gibbs, F.A. & Gibbs, E.L. (1950) *Atlas of Electroencephalography*, Addison-Wesley Press, Cambridge.

Johnson, L.C., Hanson, K. & Bickford, R.G. (1976) Effect of flurazepam on sleep spindles and K-complexes. *Electroencephalogr. Clin. Neurophysiol.*, **40**, 67–77.

Knoblauch, V., Kräuchi, K., Renz, C., Wirz-Justice, A. & Cajochen, C. (2002) Homeostatic control of slow-wave and spindle frequency activity during human sleep: effect of differential sleep pressure and brain topography. *Cereb. Cortex*, **12**, 1092–1100.

Martens, W.L.J. (1992) The fast time frequency transform (F.T.F.T.): a novel on-line approach to the instantaneous spectrum. *14th International Conference of the IEEE Engineering in Medicine and Biology Society*, Paris.

Martens, W.L.J. (1999) Segmentation of 'rhythmic' and 'noisy' components of sleep EEG, heart rate and respiratory signals based on instantaneous amplitude, frequency, bandwidth and phase. *1st Joint BMES / EMBS IEEE Conference*, Atlanta.

Novak, C.M., Harris, J.A., Smale, L. & Nunez, A.A. (2000) Suprachiasmatic nucleus projections to the paraventricular thalamic nucleus in nocturnal rats (Rattus norvegicus) and diurnal nile grass rats (Arviacanthis niloticus). *Brain Res.*, **874**, 147–157.

Pace-Schott, E.F. & Hobson, J.A. (2002) The neurobiology of sleep: genetics, cellular physiology and subcortical networks. *Nat. Rev. Neurosci.*, **3**, 591–605.

Rechtschaffen, A. & Kales, A. (1968) *A Manual of Standardized Terminology, Techniques and Scoring System for Sleep Stages of Human Subjects*. US Department of Health, Education and Welfare, Public Health Service, Bethesda, MD, USA.

Saper, C.B., Chou, T.C. & Scammell, T.E. (2001) The sleep switch: hypothalamic control of sleep and wakefulness. *Trends Neurosci.*, **24**, 726–731.

Sejnowski, T.J. & Destexhe, A. (2000) Why do we sleep? *Brain Res.*, **886**, 208–223.

Sherin, J.E., Shiromani, P., McCarley, R.W. & Saper, C.B. (1996) Activation of ventrolateral preoptic neurons during sleep. *Science*, **271**, 216–219.

Siapas, A.G. & Wilson, M.A. (1998) Coordinated interactions between hippocampal ripples and cortical spindles during slow-wave sleep. *Neuron*, **21**, 1123–1128.

Steriade, M., McCormick, D.A. & Sejnowski, T.J. (1993) Thalamocortical oscillations in the sleeping and aroused brain. *Science*, **262**, 679–685.

Trachsel, L., Dijk, D.J., Brunner, D.P., Klene, C. & Borbély, A.A. (1990) Effect of zopiclone and midazolam on sleep and EEG spectra in a phase-advanced sleep schedule. *Neuropsychopharmacology*, **3**, 11–18.

Weber, J.M., Schwander, J.C., Unger, I. & Meier, D. (1997) A direct ultrasensitive RIA for the determination of melatonin in human saliva: comparison with serum levels. *J. Sleep Res.*, **26**, 757.

Wei, H.G., Riel, E., Czeisler, C.A. & Dijk, D.J. (1999) Attenuated amplitude of circadian and sleep-dependent modulation of electroencephalographic sleep spindle characteristics in elderly human subjects. *Neurosci. Lett.*, **260**, 29–32.

Werth, E., Achermann, P., Dijk, D.J. & Borbély, A.A. (1997) Spindle frequency activity in the sleep EEG: individual differences and topographic distribution. *Electroencephalogr. Clin. Neurophysiol.*, **103**, 535–542.

Zeitlhofer, J., Gruber, G., Anderer, P., Asenbaum, S., Schimicek, P. & Saletu, B. (1997) Topographic distribution of sleep spindles in young healthy subjects. *J. Sleep Res.*, **6**, 149–155.

Zygierewicz, J., Blinowska, K.J., Durka, P.J., Szelenberger, W., Niemcewicz, S. & Androsiuk, W. (1999) High resolution study of sleep spindles. *Clin. Neurophysiol.*, **110**, 2136–2147.